DYNAMIC BUCKLING ESTIMATES*

by

John W. Hutchinson and Bernard Budiansky
Harvard University, Cambridge, Massachusetts

ABSTRACT

Attention is focused on the dynamic buckling of imperfection-sensitive models subjected to loading histories characterized by a finite length of time of load application. Results are presented which show that for all but highly imperfect structures the finite-time buckling impulse can be considerably less than the zero-time buckling impulse. The application of the results obtained from the models to actual imperfection-sensitive structures is discussed and results are obtained which suggest what would seem to be conservative buckling estimates for a long cylindrical shell loaded in axial compression and having sufficiently strong end restraints.

*This work was supported in part by the National Aeronautics and Space Administration under Grant NsG-559, and by the Division of Engineering and Applied Physics, Harvard University.

DYNAMIC BUCKLING ESTIMATES*

John W. Hutchinson and Bernard Budiansky
Harvard University, Cambridge, Massachusetts

INTRODUCTION

The buckling of imperfection-sensitive structures such as cylindrical shells under axial compression and spherical shells subject to uniform pressure has been studied intensively in recent years. While the static buckling of such structures is fairly well understood, a clear understanding of dynamic buckling is lacking. Existing analyses, as yet, hardly provide any general guidelines for design against dynamic buckling. The present paper continues the study initiated in Reference (1) with a view toward presenting a complete picture of the dynamic buckling of some imperfection-sensitive models. That initial study was concerned with buckling of the models, and real structures as well, subjected to step loadings, i.e., loads suddenly applied and subsequently held constant. Here consideration is extended to loading histories characterized by a finite length of time of load application. In addition to the presentation of results for the models, the application of these results to actual imperfection-sensitive structures is discussed and attention is focused on the cylindrical shell under axial compression.

SIMPLE MODELS: STATIC BUCKLING

The imperfection-sensitive model shown in Figure 1 is a modified version of that employed by Karman, Dunn and Tsien[2] in their early study of cylinder

---

* This work was supported in part by the National Aeronautics and Space Administration under Grant NsG-559, and by the Division of Engineering and Applied Physics, Harvard University.

buckling. The three-hinge, rigid-rod model is laterally constrained by a non-linear softening spring, and a mass M is concentrated at the hinge joining the two rods. The initial imperfection is identified with the deviation of the unloaded structure from the straight configuration. Two variations of the basic structure are investigated. The force of the constraining spring of the quadratic model is given by

$$F = kL\left[\frac{x}{L} - \alpha\left(\frac{x}{L}\right)^2\right]$$

where x is the lateral displacement. (Note that the total displacement is then $x + \bar{x}$, where the initial imperfection is $\bar{x}$.) The spring force of the cubic model is expressed as

$$F = kL\left[\frac{x}{L} - \beta\left(\frac{x}{L}\right)^3\right]$$

The equation of dynamic equilibrium for the quadratic model is

$$\ddot{z} + (1-\lambda/\lambda_C)z - \bar{\xi}\, z^2 = \lambda/\lambda_C \qquad (1)$$

and for the cubic model is

$$\ddot{z} + (1-\lambda/\lambda_C)z - \bar{\zeta}\, z^3 = \lambda/\lambda_C \qquad (2)$$

where $z = x/\bar{x}$, $\bar{\xi} = \alpha\bar{x}/L$, $\bar{\zeta} = \beta(\bar{x}/L)^2$, and $(\dot{}) \equiv \frac{1}{\omega}\frac{d}{dt}$ where $\omega = (k/M)^{1/2}$ is the vibration frequency of the unloaded structure. The static buckling load of the perfect column, the classical buckling load, is $\lambda_C = kL/2$.

The static buckling load of the imperfect structure is defined to be the maximum value obtained by the applied load and is denoted by λ_S. The static load-deflection curve for the quadratic model is shown in Figure 2(a). The maximum value of λ is obtained when $\frac{d\lambda}{dz} = 0$, and this condition used in conjunction with Equation (1) (with $\ddot{z} = 0$) yields

$$(1-\lambda_S/\lambda_C)^2 = 4\bar{\xi}\,\lambda_S/\lambda_C \qquad (3)$$

Only for $\bar{\xi} > 0$ will there be a real value of λ_S that satisfies (3); for $\bar{\xi} < 0$ there is no static buckling load.

Figure 2(b) displays the static load-deflection curve for the cubic model. A maximum value of λ occurs only if $\beta > 0$ -- the condition for the model to exhibit imperfection-sensitivity. The static buckling load of the cubic model satisfies

$$(1-\lambda_S/\lambda_C)^{3/2} = \frac{3(3\bar{\zeta})^{1/2}}{2}\,\lambda_S/\lambda_C \qquad (4)$$

DYNAMIC BUCKLING OF MODELS

Two classes of loading histories will be considered in this paper. Rectangular loading (Figure 3(a)) is characterized by λ^0, the value of applied load, and T, the length of time of load application. A particular triangular loading (Figure 3(b)) is specified by λ^0, the initial, and thus peak, value of the applied load and T. The dynamic response of either of the two models is such that (for a fixed value of T) for λ^0 less than a certain value, call it λ_D, the response is bounded, while it is unbounded for λ^0 greater than λ_D. Thus, λ_D is the natural definition of the dynamic buckling load for the models. The unbounded behavior of the dynamic response is related to the fact that the static equilibrium curve falls monotonically once the buckling load has been attained. This curve does not decrease to a minimum value of λ and then rise, as is characteristic of an actual structure.

The dynamic buckling loads for the case of step loading (the loading displayed in Figure 3(a) with $T = \infty$) were obtained in Reference (1). For the quadratic model the dynamic buckling load is related to the imperfection

parameter $\bar{\xi}$ by an expression similar in form to that for the static buckling load, namely

$$(1-\lambda_D/\lambda_C)^2 = \frac{16}{3}\,\bar{\xi}\,\lambda_D/\lambda_C \tag{5}$$

The analogous expression for the cubic model is

$$(1-\lambda_D/\lambda_C)^{3/2} = \frac{3(6\bar{\zeta})^{1/2}}{2}\,\lambda_D/\lambda_C \tag{6}$$

An expression relating λ_D to λ_S (rather than $\bar{\xi}$) is obtained by combining Equations (3) and (5) so that

$$\frac{3}{4}\left(\frac{\lambda_C-\lambda_D}{\lambda_C-\lambda_S}\right)^2 = \frac{\lambda_D}{\lambda_S} \tag{7}$$

The dynamic buckling load of the cubic model is related to the static buckling load in a similar manner by

$$\frac{1}{\sqrt{2}}\left(\frac{\lambda_C-\lambda_D}{\lambda_C-\lambda_S}\right)^{3/2} = \frac{\lambda_D}{\lambda_S} \tag{8}$$

Curves of λ_D/λ_S vs. λ_S/λ_C for the two models are displayed in Figure 4. In this form, explicit dependence on the magnitude of the imperfection has been eliminated but is reflected in λ_S/λ_C. Thus, the implications of the model results for real structures is most easily seen.

For rectangular loadings of finite duration expressions analogous to (7) and (8) (but considerably more complicated) relating λ_D, λ_S, λ_C and the additional parameter T are derived in the Appendix (see Equations (A7) and (A9)); these results also involve the vibration period of the unloaded structure $T_0 = 2\pi/\omega$. Similar analytic expressions could not be found for triangular loading, and so it was necessary for this case to resort to numerical integration of the differential equations (1) and (2) in order to discern the dynamic buckling loads λ_D. In fact, as a matter of convenience,

most of the results for rectangular loading were also found by this procedure, outlined in the Appendix.

A typical set of results is presented in Figure 5 to facilitate comparison between the two models for buckling under rectangular loading. For the case $\lambda_S/\lambda_C = .5$ Figure 5 displays curves of λ_D/λ_S vs. T/T_0 for each model. For a given value of T/T_0 the cubic model buckles at a lower load than the quadratic. For large T/T_0, λ_D/λ_S approaches the value predicted by either Equation (7) or (8).

Figures 6(a) and (b) essentially summarize all the data for buckling under rectangular loading. These figures display curves of λ_D/λ_S vs. λ_S/λ_C for various values of T/T_0. In this form the data is presented in the same spirit as in Figure 4, i.e., the dynamic buckling load of the structure is related to its static buckling load. The lowest curves in Figures 6(a) and 6(b), corresponding to $T/T_0 = \infty$, are those presented in Figure 4.

Figures 7(a) and (b) are plotted in the same manner as Figure 6 but for the case of triangular loading. The general features of these curves are similar to those of Figure 6. For triangular as well as rectangular loading λ_D/λ_S approaches the value given by either (7) or (8) for large T/T_0.

The finite-time buckling impulse is $I = \frac{1}{2}\lambda_D T$ for rectangular loading, and $I = \frac{1}{2}\lambda_D T$ for triangular loading. The zero-time buckling impulse for the quadratic model (given in Reference (1)) is

$$I_0 = \frac{2(3)^{-1/2}}{\pi}\lambda_S T_0 (1-\lambda_S/\lambda_C)^{-2} \qquad (9)$$

and for the cubic model is readily found to be

$$I_0 = \frac{3(6)^{1/2}}{8\pi}\lambda_S T_0 (1-\lambda_S/\lambda_C)^{-3/2} \qquad (10)$$

Thus I/I_0 depends only on T/T_0 and λ_S/λ_C ; and these results for each model, for both rectangular and triangular loading, are given in Figure 8. Over the range of T/T_0 plotted the buckling impulse required for triangular loading does not differ appreciably from that associated with rectangular loading. It is noted that for all but highly imperfect structures the finite-time buckling impulse can be considerably less than the zero-time buckling impulse.

APPLICATION OF THE SIMPLE-MODEL RESULTS

Before attempting to discuss the application of the above results to real structures we can make three observations of a qualitative nature which follow from the simple-model results. Firstly, it is seen in Figure 6 that for any given value of T/T_0 there is a large variation of λ_D/λ_S over the possible range of λ_S/λ_C . Clearly, the more imperfect the structure the smaller is λ_D/λ_S . The simple-model results strongly suggest that one should expect even more scatter in experimental results on dynamic buckling than has been noted in conjunction with static buckling tests. The second observation is related to the first but seems worthy of separate notice. For nearly perfect structures, that is when λ_S/λ_C is almost unity, the indication is that there is a possibility of dynamic buckling loads several times larger than the static buckling load even for loads which are applied for times comparable with the natural vibration period of the unloaded structure. The third comment, already made in regard to Figure 8, is that the finite-time impulse necessary for buckling can be significantly less than zero-time buckling impulse. The zero-time buckling impulse is only a safe estimate for the finite-time impulse when the structure is highly imperfect.

Buckling under step loading of actual imperfection-sensitive structures

was investigated in Reference (1) by means of an extension of Koiter's general theory of elastic stability[3] to include inertial effects. General equilibrium equations were obtained such that the load parameter was related to the deflection of the structure in the buckling mode (or modes) associated with lowest buckling eigenvalue of the linear buckling analysis. For some special classes of structures the general equilibrium equations reduced to either Equations (1) or (2) and hence one or the other of the curves in Figure 4 was directly applicable. For certain other structures (including the cylindrical shell under axial load) it appeared that the lower curve in Figure 4 should provide a conservative estimate of dynamic buckling under step loading.

When the length of time of load application is very short so that the dynamic buckling load is large compared to the classical buckling load (the buckling load of the perfect structure) it is much more difficult to justify the applicability of the model results. Two necessary conditions for their validity are (1) that the inertia associated with the prebuckling mode of deformation of the perfect structure be negligible and (2) that the dynamic buckling mode of the structure be not appreciably different from the static buckling mode.

Application of the model results to an imperfection-sensitive structure necessitate: (1) assignment of a value to $T_0 \equiv 2\pi/\omega$ and (2) specification of the nature of the structure -- quadratic or cubic. If the buckling mode of the structure is a vibration mode as well, the first requirement can be met if ω is associated with the vibration frequency of this mode. A structure which deforms in a number of buckling modes, such as the cylindrical shell under axial compression, presents difficulties in this respect. A

conservative choice may lead to identifying ω with the largest of the buckling mode frequencies.

For a given time of load application T/T_0, the lowest value of λ_D/λ_S for either model is that corresponding to the limiting case $\lambda_S/\lambda_C = 0$ (see Figures 6 and 7). These limiting relations provide a conservative estimate of λ_D/λ_S vs. T/T_0. In situations in which the possibility of small values of λ_S/λ_C cannot be discounted the use of these conservative relations between λ_D/λ_S and T/T_0 may be appropriate. For convenience, the variations of λ_D/λ_S with T_0/T for rectangular loading for the case $\lambda_S/\lambda_C = 0$ are plotted in Figure 9. For small T_0/T the value of λ_D/λ_S approaches that for step loading, i.e., 3/4 for the quadratic model and $2^{-1/2}$ for the cubic model. If T_0/T is large the behavior approaches the zero-time impulse situation, and from Equations (9) and (10) the product $\frac{\lambda_D}{\lambda_S}\frac{T}{T_0}$ approaches $2/\pi(3)^{1/2}$ for the quadratic model and $3(6)^{1/2}/8\pi$ for the cubic model. As previously noted, the cubic model estimates are below those for the quadratic model. Analytic expressions for these limiting cases are given in the Appendix.

THE LONG CYLINDRICAL SHELL UNDER AXIAL LOAD

In what follows, we have no intention of presenting anything but a crude analysis of the axially loaded cylindrical shell, the imperfection-sensitivity of which is associated with a multiplicity of buckling modes. The results, nevertheless, tend to substantiate the general applicability of the results for the models. On the basis of these results we are led to suggest what would seem to be conservative buckling estimates for the cylindrical shell under axial compression.

The classical buckling stress of a long cylindrical shell under axial

compression having sufficiently strong end constraints is

$$\lambda_C = (3(1-\nu^2))^{-1/2} \frac{Eh}{R}$$

where E is Young's modulus, ν is Poisson's ratio, R is the shell radius and h is the shell thickness. Following the treatment given in Reference (1), we restrict consideration to only two of the many buckling modes associated with this critical stress. In particular, we assume that the buckling deformation of the shell takes place in its axisymmetric buckling mode and in the non-axisymmetric mode with axial buckle wave-length twice that of the axisymmetric mode.

The following two equilibrium equations were obtained in Reference (1) on the basis of the previously mentioned extension of Koiter's general theory:

$$\frac{1}{4} \ddot{\xi}_1 + (1-\lambda/\lambda_C)\xi_1 - \frac{3c}{32} \xi_2^2 = \lambda/\lambda_C \bar{\xi}_1 \qquad (11)$$

$$\ddot{\xi}_2 + (1-\lambda/\lambda_C)\xi_2 - \frac{3c}{2} \xi_1 \xi_2 = \lambda/\lambda_C \bar{\xi}_2 \qquad (12)$$

where $c = (3(1-\nu^2))^{1/2}$. Here, ξ_1 is the deflection (relative to the shell thickness) of the shell in its axisymmetric buckling mode; similarly, ξ_2 is the deflection in the non-axisymmetric mode. The initial imperfections in the cylindrical geometry of the shell are taken to be in the form of the two buckling modes and are of amplitude $\bar{\xi}_1$ and $\bar{\xi}_2$ relative to the shell thickness. Finally, we have let $\dot{(\,)} = \frac{1}{\omega^{(2)}} \frac{d(\,)}{dt}$ where the vibration frequencies associated with the two modes (axial and circumferential inertias neglected) are

$$\omega^{(1)} = \frac{1}{R}\left(\frac{2E}{\rho}\right)^{1/2} \quad \text{and} \quad \omega^{(2)} = \frac{1}{R}\left(\frac{E}{2\rho}\right)^{1/2}$$

The buckling behavior of the cylinder under axially applied step loading was studied in Reference (1) with the aid of the above two equilibrium equations. Curves of λ_D/λ_S vs. λ_S/λ_C were obtained for a variety of

ratios of $\bar{\xi}_1$ to $\bar{\xi}_2$ -- i.e., relative amount of axisymmetric to non-axisymmetric imperfection. The smallest value of λ_D/λ_S for any given value of λ_S/λ_C was found to correspond to combinations of $\bar{\xi}_1$ and $\bar{\xi}_2$ such that the axisymmetric imperfection was zero, $\bar{\xi}_1 = 0$. A good approximation to this case can be obtained analytically if the inertia term, $\frac{1}{4}\ddot{\xi}_1$, in Equation (11) is neglected. With this approximation, Equations (11) and (12) can be combined to give

$$\ddot{z}_2 + (1-\lambda/\lambda_C)z_2 - \frac{\gamma}{(1-\lambda/\lambda_C)} z_2^3 = \lambda/\lambda_C \qquad (13)$$

where $z_2 = \xi_2/\bar{\xi}_2$ and $\gamma = \frac{9c^2}{64}\bar{\xi}_2^2$. Although this equation is not identical to the equation for the cubic model, it is strikingly similar.

For the case of <u>step loading</u> the dynamic buckling stress is related to the static buckling stress of the imperfect structure by

$$\frac{1}{\sqrt{2}}\left(\frac{\lambda_C-\lambda_D}{\lambda_C-\lambda_S}\right)^2 = \frac{1}{2}\frac{\lambda_D}{\lambda_S} \qquad (14)$$

This formulas was given in Reference (1) and the results are between those for the two models.

No attempt has been made to make a complete study with either Equations (11) and (12) or Equation (13) for dynamic buckling of the cylinder under rectangular loading. However, we do present two results, using Equation (13), which tend to reinforce predictions based on the simple models. The zero-time impulse necessary to buckle the cylinder is

$$I_0 = \lim_{T\to 0} \lambda_D T = \frac{3(6)^{1/2}}{8\pi}\lambda_S T_0\left(1 - \frac{\lambda_S}{\lambda_C}\right)^{-2} \qquad (15)$$

where $T_0 = 2\pi/\omega^{(2)}$. For all values of λ_S/λ_C , this gives values of $I_0/\lambda_S T_0$ for the cylinder between the predictions for the two models as given by Equations (9) and (10).

Secondly, and perhaps more important from the standpoint of design, the relation between λ_D/λ_S and T_0/T for rectangular loading for the limiting case $\lambda_S/\lambda_C = 0$ can be shown to be identical to that for the cubic model. Recall that this relation is given in the Appendix and is plotted in Figure 9.

Thus we seem to be led to the same conservative estimate for λ_D/λ_S vs. T/T_0 as was obtained for the cubic model. It is well known that values of λ_S/λ_C for cylindrical shells under axial compression are often as little as .25; thus, design on the basis of the limiting case $\lambda_S/\lambda_C = 0$ may not be unduly conservative. The value of T_0 is

$$T_0 = 2\pi/\omega^{(2)} = 2\pi R\left(\frac{2\rho}{E}\right)^{1/2}$$

but one is tempted to suggest an even more conservative criterion on the basis of the argument that $\omega^{(2)}$ really has no special significance since it emerged as a result of our restriction to only one non-axisymmetric buckling mode. Among all the static buckling modes of the shell, the vibration period of the axisymmetric mode is the smallest. The choice of

$$T_0 = 2\pi/\omega^{(1)} = 2\pi R\left(\frac{\rho}{2E}\right)^{1/2}$$

in conjunction with the results in Figure 9 for the cubic model provides what would seem to be a conservative dynamic buckling criterion.

We end this section on a note of caution. Equations (11) and (12) as well as (13) are obtained under the assumption that the dynamic buckling modes are the same as the static buckling modes. This would seem to be a reasonable assumption as long as the applied stress λ is not significantly greater than λ_C. However, for shorter lengths of time of load application and consequently larger values of applied axial stress one must not overlook the possibility of buckling in modes which are not characteristic of static

buckling. This possibility has not been accounted for in the present analysis.

APPENDIX: ANALYSIS OF SIMPLE MODELS

Here we present an analytic procedure for obtaining the buckling load of the quadratic model under rectangular loading. The results for the cubic model can be found in a similar manner.

Analytic Procedure (Rectangular Loading)

The equation of dynamic equilibrium for the quadratic model is

$$\ddot{z} + (1-\lambda/\lambda_C)z - \bar{\xi}\, z^2 = \lambda/\lambda_C \qquad \text{(A1)}$$

where $\bar{\xi} = \alpha \frac{\bar{x}}{L}$ and $(\dot{}) = \frac{1}{\omega}\frac{d}{dt}$. A first integral can be obtained for the case of λ suddenly applied for a length of time $\bar{T}$. One finds

$$\dot{z}^2 + (1-\lambda/\lambda_C)z^2 - \frac{2}{3}\bar{\xi}\, z^3 = 2\,\lambda/\lambda_C\, z \qquad \text{for} \qquad t < \bar{T} \qquad \text{(A2)}$$

and

$$\dot{z}^2 + z^2 - \frac{2}{3}\bar{\xi}\, z^3 = \lambda/\lambda_C(2\bar{z} + \bar{z}^2) \qquad \text{for} \qquad t > \bar{T} \qquad \text{(A3)}$$

for the initial conditions $z = \dot{z} = 0$ at $t = 0$ and where $\bar{z}$ denotes the value of z at $t = \bar{T}$.

The dynamic buckling load λ_D for any given value of time of load application $\bar{T}$ has been defined as the maximum value of λ such that the response remains bounded. The analysis is simplified if we adopt an equivalent but slightly different point of view. Applying a load λ we look for the maximum value of $\bar{T}$, call it $\bar{T}_D$, such that the response remains bounded.

Figure A1 depicts schematically, in the $(z,\dot{z})$ phase plane, a series of responses for several values of $\bar{T}$ for one given value of λ. When the response is bounded, that is for any $\bar{T} < \bar{T}_D$, z attains a maximum z_m

when $\dot{z} = 0$ and this value occurs for $t > \bar{T}$. By Equation (A3)

$$z_m^2 - \frac{2}{3}\bar{\xi}\, z_m^3 = \lambda/\lambda_C(2\bar{z} + \bar{z}^2) \tag{A4}$$

For all responses for which $\bar{T} < \bar{T}_D$, $\ddot{z} < 0$ when $z = z_m$; but for $\bar{T} = \bar{T}_D$, $\ddot{z} = 0$ when $z = z_m$ and by Equation (A1)

$$z_m - \bar{\xi}\, z_m^2 = 0$$

or

$$z_m = \frac{1}{\bar{\xi}} \tag{A5}$$

Now the value of $\bar{z}$ associated with the maximum bounded response can be obtained from Equations (A4) and (A5). This is

$$\bar{z}_D = \left(1 + \frac{1}{3\bar{\xi}^2}\frac{\lambda_C}{\lambda}\right)^{1/2} - 1 \tag{A6}$$

The value of $\bar{T}$ associated with the maximum bounded response, $\bar{T}_D$, is found by integrating Equation (A2); this gives, finally, for the quadratic model,

$$\frac{T}{T_0} = \frac{1}{2\pi}\int_0^{\bar{z}_D}\left(2\frac{\lambda_D}{\lambda_C}z - \left(1 - \frac{\lambda_D}{\lambda_C}\right)z^2 + \frac{2}{3}\bar{\xi}\, z^3\right)^{-1/2} dz \tag{A7}$$

where $T_0 = 2\pi/\omega$, and, consistent with the notation in the body of the paper, T has been identified with $\bar{T}_D$ and λ with λ_D. Note that $\bar{\xi}$ can be expressed in terms of λ_S/λ_C (see Equation (3)).

The relation of λ_D/λ_S to T/T_0 for the limiting case $\lambda_S/\lambda_C = 0$ may be useful as a conservative buckling criterion. For small λ_S/λ_C

$$\bar{\xi} \approx \frac{1}{4}\frac{\lambda_C}{\lambda_S}$$

and

$$\bar{z}_D \approx \frac{8}{3}\frac{\lambda_S}{\lambda_C}\frac{\lambda_S}{\lambda_D}$$

In the limit as λ_S/λ_C approaches zero (A7) becomes, with an appropriate change of the variable of integration,

$$\frac{T}{T_0} = \frac{2(3)^{-1/2}}{\pi} \frac{\lambda_S}{\lambda_D} \int_0^1 \left(1 - \frac{4}{3}\left(\frac{\lambda_S}{\lambda_D}\right)^2 \zeta^2 + \frac{16}{27}\left(\frac{\lambda_S}{\lambda_D}\right)^3 \zeta^4\right)^{-1/2} d\zeta \qquad \text{(A8)}$$

Cubic Results (Rectangular Loading)

Analogous expressions for the cubic model, based on Equation (2), are found in a manner similar to that described for the quadratic model. The dynamic buckling load λ_D is related to the imperfection parameter $\bar{\zeta}$ (and thus, by Equation (4), to λ_S/λ_C) and T by

$$\frac{T}{T_0} = \frac{1}{2\pi} \int_0^{\bar{z}_D} \left(2 \frac{\lambda_D}{\lambda_C} z - \left(1 - \frac{\lambda_D}{\lambda_C}\right) z^2 + \frac{1}{2} \bar{\zeta} z^4\right)^{-1/2} dz \qquad \text{(A9)}$$

where here $\bar{z}_D = \left(1 + \frac{1}{2\bar{\zeta}} \frac{\lambda_C}{\lambda_D}\right)^{1/2} - 1$. The conservative buckling estimate for the cubic model corresponding to the limiting case $\lambda_S/\lambda_C = 0$ and plotted in Figure 9 is

$$\frac{T}{T_0} = \frac{3(6)^{1/2}}{8\pi} \frac{\lambda_S}{\lambda_D} \int_0^1 \left(1 - \frac{27}{32}\left(\frac{\lambda_S}{\lambda_D}\right)^2 \zeta^2 + \frac{1}{16}\left(\frac{27}{16}\right)^2 \left(\frac{\lambda_S}{\lambda_D}\right)^4 \zeta^6\right)^{-1/2} d\zeta \qquad \text{(A10)}$$

Numerical Procedure

Since expressions similar to those given for rectangular loading could not be found for triangular loading, a straightforward numerical procedure based on integration of the differential equation (A1) was derived. This procedure was actually used for most of the rectangular loading calculations as well as for triangular loading and spot checks on its accuracy were made by means of the analytic results for rectangular loading. For prescribed histories of λ the values of z and $\dot{z}$ at the time $t = T$ were calculated.

Using these values it was possible to determine, again numerically, whether the subsequent response was bounded or unbounded. Thus, repeated calculations with different choices for λ were necessary to determine the critical history for a given value of T.

REFERENCES

1. Budiansky, B. and Hutchinson, J., "Dynamic Buckling of Imperfection-Sensitive Structures", to be published in Proceedings of the Eleventh International Congress of Applied Mechanics, 1964.

2. Von Karman, Th., Dunn, L. G. and Tsien, H. S., "The Influence of Curvature on the Buckling Characteristic of Structures", J. Aero. Sci., Vol. 7, No. 7, 1940.

3. Koiter, W. T., "Elastic Stability and Post Buckling Behavior", in Non Linear Problems, edited by Langer, R. E., University of Wisconsin Press, 1963.

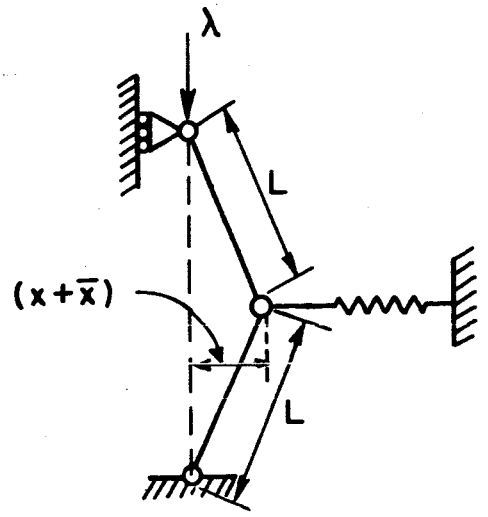

IDEALIZED COLUMN CONSTRAINED
BY NON-LINEAR SPRING

Fig. 1

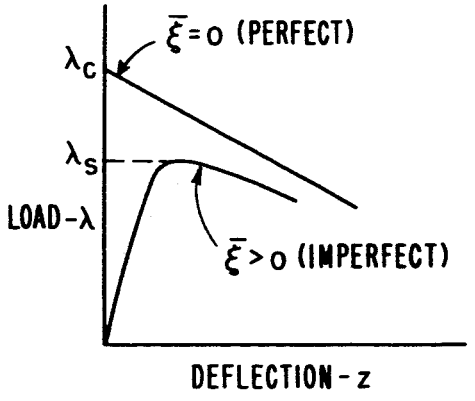

Fig. 2 (a) QUADRATIC MODEL

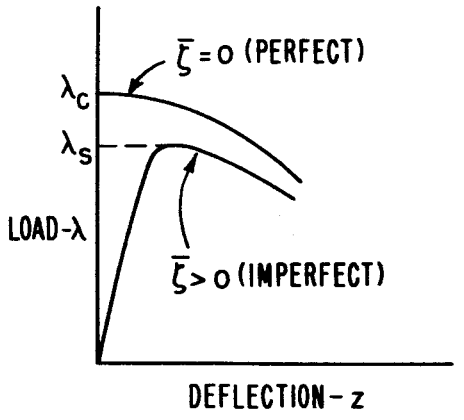

Fig. 2 (b) CUBIC MODEL

STATIC LOAD-DEFLECTION CURVES

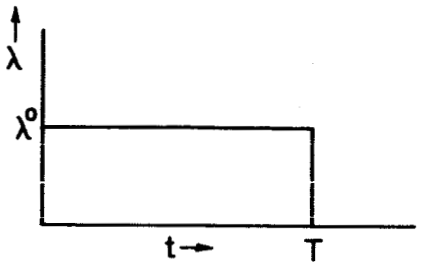

RECTANGULAR LOADING

Fig. 3a

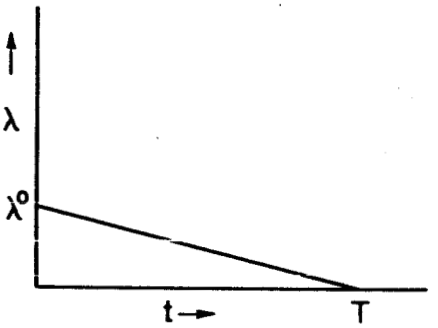

TRIANGULAR LOADING

Fig. 3b

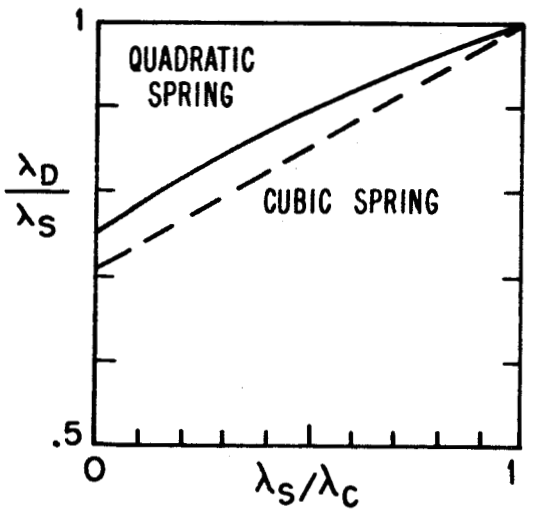

DYNAMIC BUCKLING LOADS OF SIMPLE MODELS ; STEP LOADING

Fig. 4

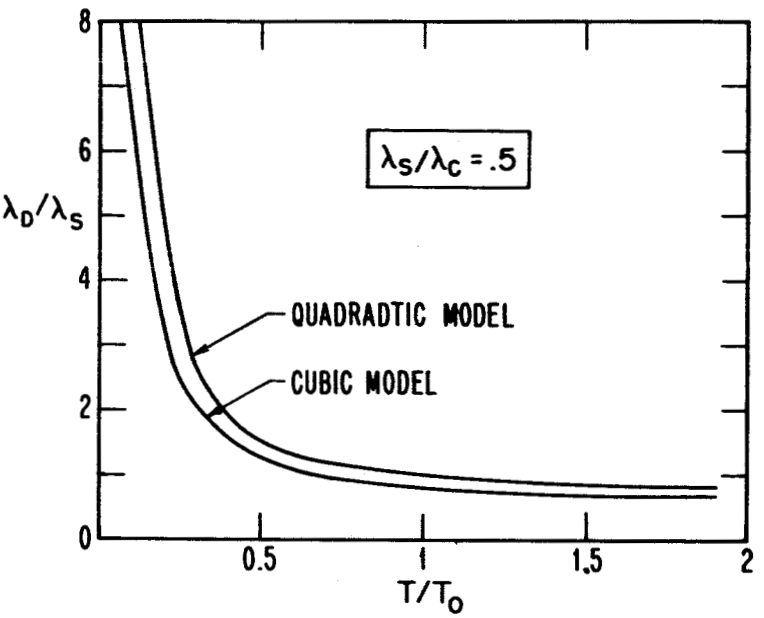

BUCKLING OF IMPERFECT MODEL UNDER RECTANGULAR LOADING

Fig. 5

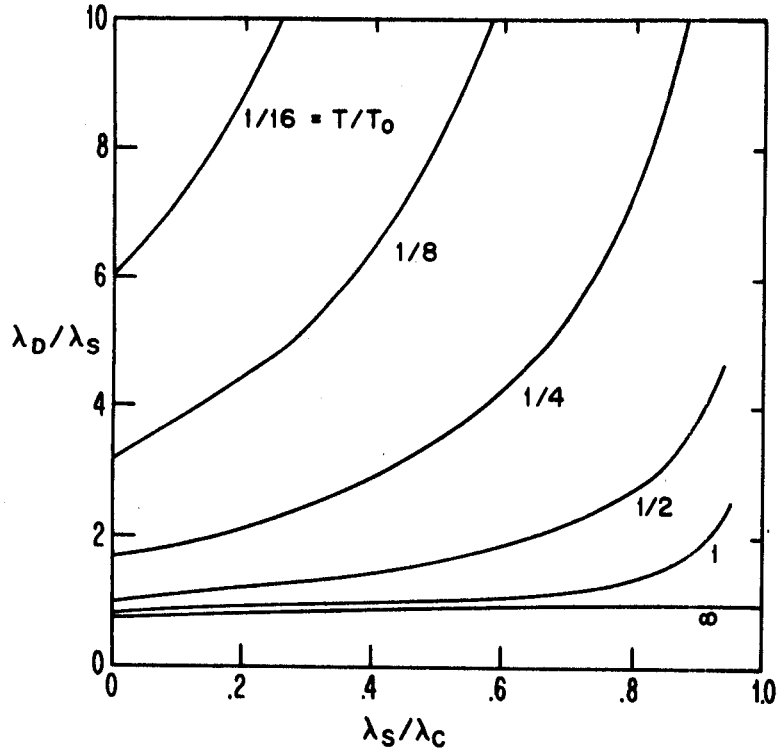

QUADRATIC MODEL: BUCKLING UNDER RECTANGULAR LOADING

Fig. 6a

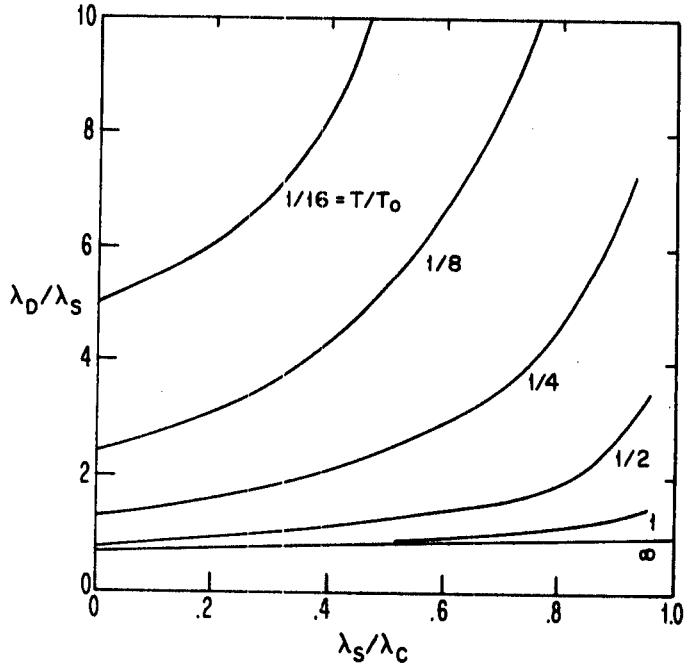

CUBIC MODEL: BUCKLING UNDER RECTANGULAR LOADING

Fig. 6b

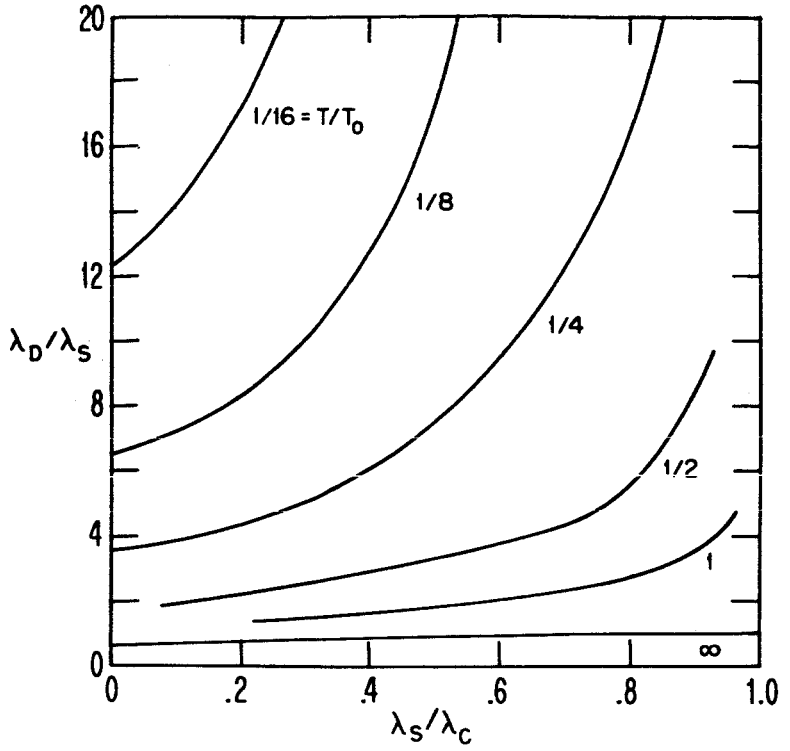

QUADRATIC MODEL: BUCKLING UNDER TRIANGULAR LOADING

Fig. 7a

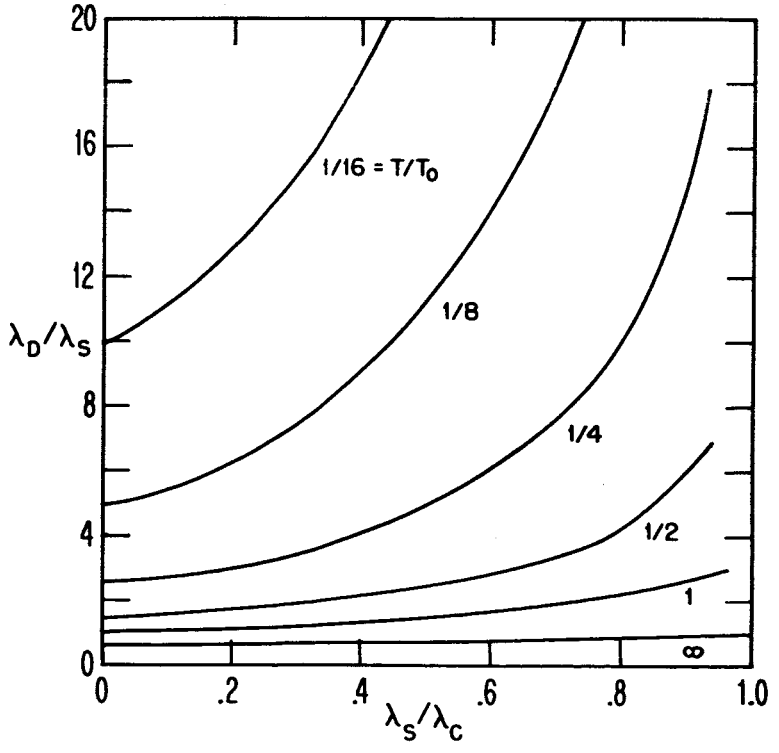

CUBIC MODEL: BUCKLING UNDER TRIANGULAR LOADING

Fig. 7b

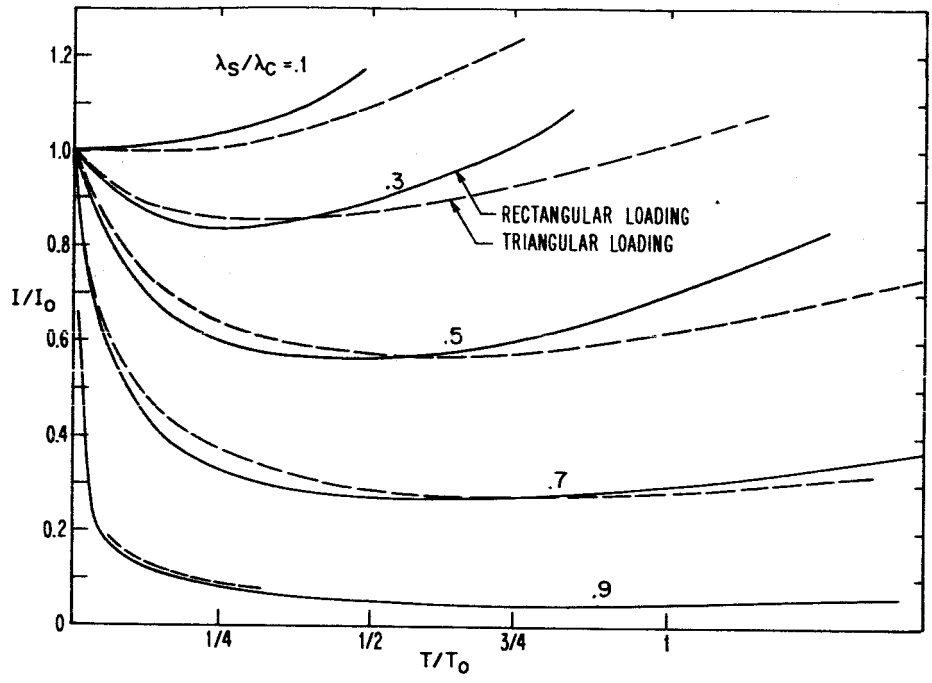

QUADRATIC MODEL: FINITE-TIME BUCKING IMPULSE
Fig. 8a

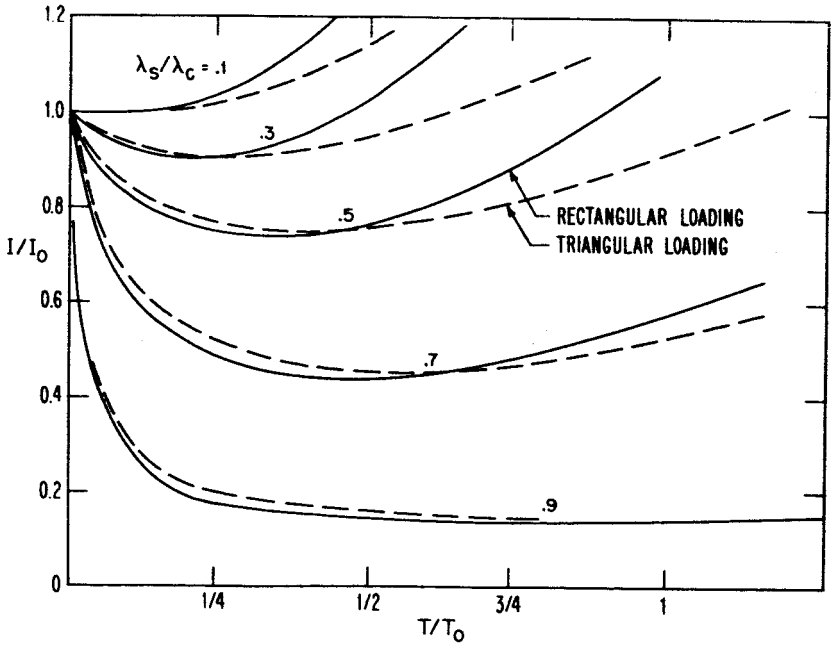

CUBIC MODEL: FINITE-TIME BUCKLING IMPULSE
Fig. 8b

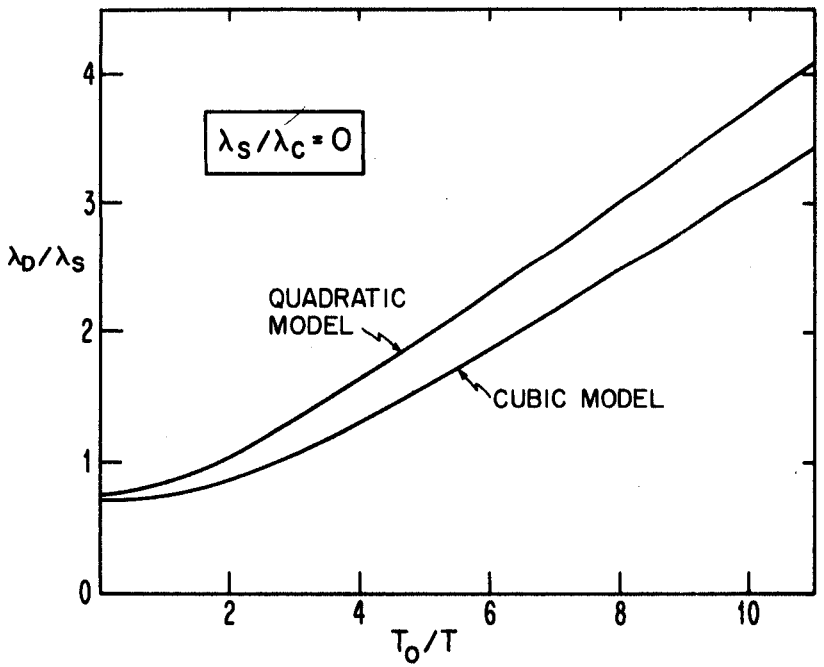

CONSERVATIVE BUCKLING ESTIMATES
RECTANGULAR LOADING

Fig. 9

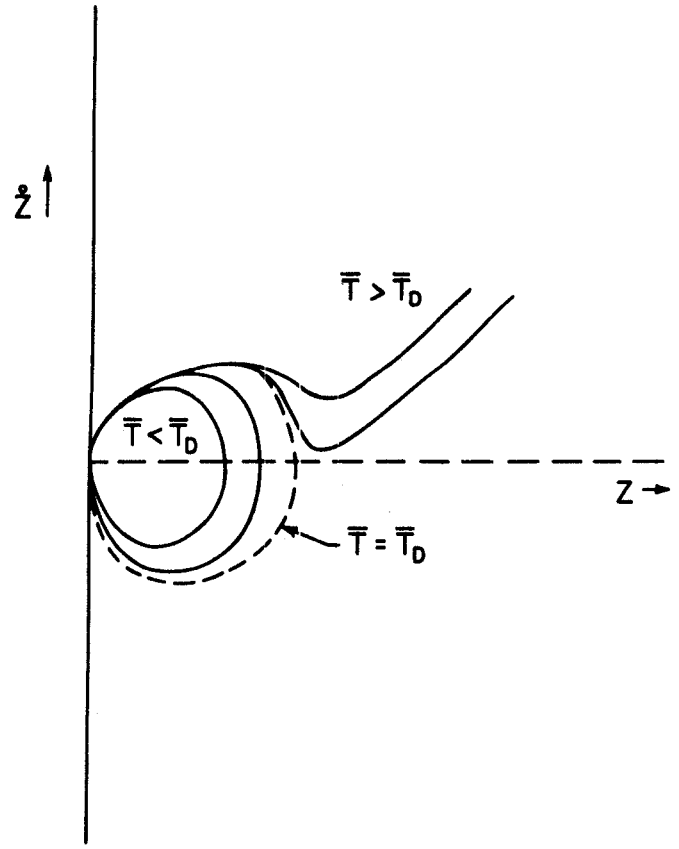

Fig. A-1